Sequential Forward S_2-S_2 and Back S_1-S_1 (Cyclic) Energy Transfer in a Novel Azulene−Zinc Porphyrin Dyad

Edwin K. L. Yeow,*,† Marcin Ziolek,‡ Jerzy Karolczak,‡,⊥ Sergey V. Shevyakov,§ Alfred E. Asato,§ Andrzej Maciejewski,‡,|| and Ronald P. Steer*,†

Department of Chemistry, University of Saskatchewan, Saskatoon, Saskatchewan, Canada S7N 5C9, Center for Ultrafast Laser Spectroscopy, Adam Mickiewicz University, Umultowska 85, 61-614 Poznan, Poland, Faculty of Physics, Adam Mickiewicz University, Umultowska 85, 61-614 Poznan, Poland, Faculty of Chemistry, Adam Mickiewicz University, Grunwaldzka 6, 60-780 Poznan, Poland, and Department of Chemistry, University of Hawaii, 2545, The Mall, Honolulu, Hawaii 96822

Received: August 3, 2004; In Final Form: September 23, 2004

A covalently tethered dyad containing the azulene (Az) and zinc tetraphenylporphyrin (ZnP) chromophores has been synthesized and its excited-state dynamics investigated, using the tether-substituted monochromophoric species as reference compounds. One photon excitation of the dyad at 270 nm results in selective population of the S_2 state of the azulene moiety, followed by near-quantitative electronic relaxation in the cycle $S_2(Az)-S_2(ZnP)-S_1(ZnP)-S_1(Az)-S_0$. Energy transfer from the S_2 state of the azulene moiety to the S_2 state of the ZnP moiety is ultrafast ($k_{eet} > 2 \times 10^{12}$ s^{-1}) and quantitative. The ZnP(S_2) moiety subsequently undergoes rapid ($k_{ic} = 3 \times 10^{11}$ s^{-1}), quantitative internal conversion to its S_1 state. Thereafter, the excitation residing on the S_1 state of the ZnP is returned to the Az moiety via an efficient (ca. 90%) back S_1-S_1 energy transfer process ($k_{eet} = 2.8 \times 10^9$ s^{-1}). Ultimately the system returns to the electronic ground state via conical intersection of the azulene S_1 and S_0 surfaces in ca. 1 ps. The cyclic interchromophoric energy transfer rates are nearly the same in both acetonitrile and cyclohexane, suggesting that the conformation of the tether is similar in both solvents. Förster theory is inadequate in explaining the efficient energy transfer dynamics, and other processes such as the Dexter mechanism must be invoked.

1. Introduction

Recent advances in optoelectronics and molecular logic gates have prompted great interest in the photophysics and photochemistry of polyatomic molecules with relatively long-lived highly excited electronic states.[1] Azulene and metalloporphyrins (e.g., zinc tetraphenylporphyrin), known to violate Kasha's rule, are photochemically stable and therefore act as potential candidates for the design of efficient molecular logic devices. Azulene exhibits relatively intense fluorescence from its S_2 state, while undergoing an ultrafast internal conversion from its S_1 to S_0 states via conical intersection.[2] On the other hand, many diamagnetic metalloporphyrins display weak S_2-S_0 fluorescence as a result of the modest energy gap (∼0.8 eV) between their S_2 and S_1 states.[3]

Levine and co-workers have succinctly described the opportunity to utilize energy transfer between higher electronic states to achieve more efficient molecular logic gates and circuits.[4] This arises from the need to use a greater number of states per molecule (say, both S_1 and S_2 states) for logic operations. We have previously proposed the design of an efficient molecular logic circuit based on sequential forward S_2-S_2 energy transfer and back S_1-S_1 energy transfer (i.e., cyclic energy transfer) for a system comprising an azulene and a zinc porphyrin.[5] Due to significant spectral overlap between the S_2 emission spectrum of azulene and the S_2 absorption spectrum of zinc porphyrin, resonance S_2-S_2 energy transfer from azulene to zinc porphyrin can take place. Furthermore, an overlap between the S_1 emission spectrum of zinc porphyrin and the S_1 absorption spectrum of azulene allows back S_1-S_1 energy transfer to occur after the S_1 state of the zinc porphyrin is produced by rapid internal conversion from its S_2 level.

S_2-S_2 energy transfer between azulene and zinc porphyrin has been investigated in dichloromethane and cetyl trimethyl ammonium bromide (CTAB) micelles.[6] In dichloromethane, an efficient transfer of energy, which cannot be rationalized using Förster theory alone, is observed and was attributed to an inhomogeneous distribution of the azulene donor molecules surrounding the energy-accepting zinc porphyrins. Other mechanisms, such as short-range exchange interaction and higher multipole interaction, were shown to be important. On the other hand, the Förster mechanism was found to agree well with the experimental energy transfer efficiency when azulene and zinc porphyrin are encapsulated in CTAB micelles.

Herein, we report the synthesis of a covalently tethered azulene−zinc porphyrin dyad (Az−ZnP) and determine its photophysical properties in two solvents of different polarity, acetonitrile and cyclohexane. The desired cyclic energy transfer process is shown to occur with high efficiency. This study provides useful insight into the factors that control the cyclic energy transfer process and forms a platform for further studies involving the incorporation of such species into molecular devices.

* Corresponding authors. Fax: +1-306-966-4730. E-mail addresses: eky341@duke.usask.ca (E. K. L. Yeow); ron.steer@usask.ca (R. P. Steer).
† University of Saskatchewan.
‡ Center for Ultrafast Laser Spectroscopy, Adam Mickiewicz University.
⊥ Faculty of Physics, Adam Mickiewicz University.
§ University of Hawaii.
|| Faculty of Chemistry, Adam Mickiewicz University.

10.1021/jp0465175 CCC: $27.50
Published on Web 11/19/2004

SCHEME 1[a]

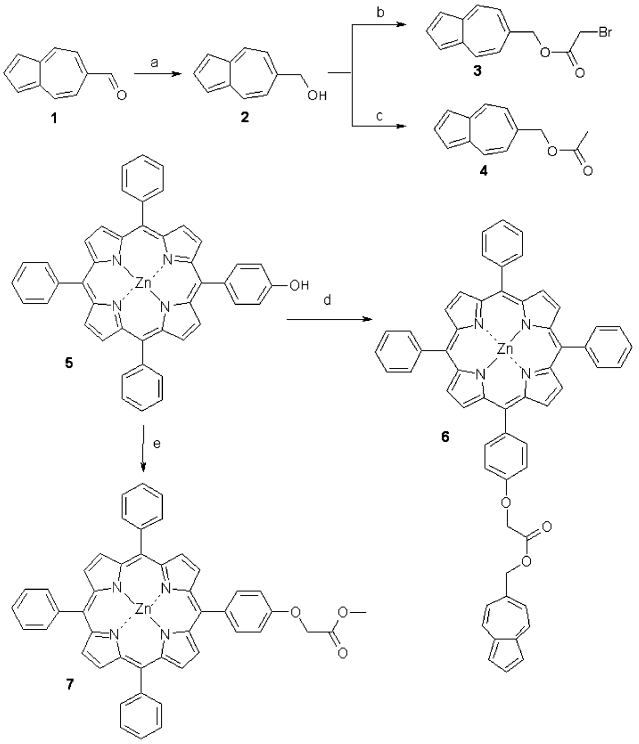

[a] Reagents and conditions: (a) $NaBH_4$, MeOH; (b) NaH, THF, $BrCH_2C(O)Cl$; (c) NaH, THF, acetyl chloride; (d) **3**, Py, CH_2Cl_2; (e) methyl bromoacetate, Py, CH_2Cl_2.

2. Experimental Section

2.1. Synthesis. Scheme 1 shows the synthetic route adopted to synthesize the azulene−zinc porphyrin dyad **6** (Az−ZnP) and the two reference compounds **4** (Az-ref) and **7** (ZnP-ref). 6-Formylazulene **1** was prepared according to the procedure of Hafner starting from *N*-butyl-4-(1,3-dioxolan-2-yl)pyridinium bromide.[7] The reduction of aldehyde **1** was performed cleanly by $NaBH_4$ in MeOH at room temperature, and the resulting alcohol **2** (yield ∼95%) was acylated with bromoacetyl chloride in THF using NaH as a base to give the corresponding bromide **3** (80% yield). Reference compound **4** was obtained in the same manner using acetyl chloride in the acetylation step (yield ∼96%).

Condensation of zinc tetrakis-5,10,15-triphenyl-20-(4-hydroxyphenyl)-21*H*,23*H*-porphyrin[8] (**5**) with the bromo-derivative of azulene **3** or with methyl bromoacetate under mild basic conditions led to the desired dyad **6** (yield ∼75%) and the reference compound **7** (yield ∼82%), respectively.

All final compounds were purified by flash chromatography on Merck silica gel 60 (80−100 mesh) using CH_2Cl_2 as a solvent. The NMR data of reference compounds **4** (Az-ref), **7** (ZnP-ref), and **6** (Az−ZnP dyad) are given in Table 1.

2.2. Spectroscopy. All measurements were performed at room temperature in acetonitrile (Merck, HPLC grade) and cyclohexane (Merck, HPLC grade). To achieve optimal experimental signal-to-noise ratios, concentrations near the solubility limit of the Az−ZnP dyad in these solvents were used. The concentrations of all compounds were ca. 4×10^{-5} M in acetonitrile and ca. 5×10^{-6} M in cyclohexane. No aggregate formation was observed.

The stationary UV/vis absorption spectra were taken with a UV−Vis-550 (Jasco) spectrophotometer. The steady-state fluorescence emission spectra were recorded with two different spectrofluorimeters: a modified Edinburgh Instruments FL 9000 and a modified MPF-3 (Perkin-Elmer). The Edinburgh Instruments spectrofluorimeter, with a laser as an excitation source, ensured high intensity and monochromaticity of the excitation beam, low levels of scattered light, and minimization of the reabsorption effect.[9] Emission quantum yields of the reference compounds were obtained using the Edinburgh Instruments spectrofluorimeter with quinine sulfate in 0.05 M aqueous H_2SO_4 as the reference standard. The modifications introduced into the MPF-3 spectrofluorimeter enabled single-photon counting detection and data processing using a dual-photon counting setup (Light-Scan). The MPF-3 spectrofluorimeter was also used to measure the fluorescence excitation spectra.

The apparatus and procedures used for the time-resolved emission measurements has been described in detail previously.[10] Briefly, the train of 1−2 ps pulses from an argon ion-pumped, tunable, mode-locked Ti:sapphire laser was pulse-picked at a frequency of 4 MHz. Second and third harmonics of these pulses were used as the excitation source for the measurement of upper state fluorescence lifetimes by time-correlated single-photon counting with an accuracy of ca. 300 fs. A graded, rotating neutral density filter was used to control the intensity of the excitation beam, and a Fresnel double rhomb was employed to rotate the plane of its polarization. Together with a polarizer set to observe emission at the magic angle, this arrangement eliminates rotational diffusion artifacts. The detector is a Hamamatsu R3809U-05 microchannel plate photomultiplier.

The equipment used for the transient absorption has previously been described in detail.[11] The output of the laser system (femtosecond titanium-sapphire) was set at a 1 kHz repetition rate providing pulses of about 100 fs duration. The probe beam passed through an optical delay line consisting of a retroreflector mounted on a computer-controlled motorized translation stage and was then converted to a white light continuum (in a 2 mm rotating calcium fluoride plate), the diameter of which was 2−5 times smaller than that of the pumping beam. A grating polychromator was used in conjunction with a thermoelectrically cooled CCD camera to record the spectra. To improve the signal-to-noise ratio, the transient absorption measurements were performed in double-beam mode (probe and reference) with two synchronized choppers in the pump and probe paths, which substantially eliminated the influence of the laser intensity fluctuations and, consequently, allowed measurements of much lower values of the optical density changes. With this experimental setup, the absorbance changes (ΔA) can be measured with an accuracy of ±0.0005 in the 300−700 nm spectral range.

The thickness of the flowing sample was 2 mm. The pulse energies for pump wavelengths of 270 and 400 nm were 2 and 10 μJ, respectively. All spectra were corrected for group velocity dispersion effects according to the standard numerical scheme.[12] The chirp of the white light continuum was obtained by measuring two-photon absorption in a very thin (150 μm) BK7 glass plate. An additional contribution to dispersion, due to the front window of the sample cell, was calculated from the Sellmeier equation. The transient absorption signals originating from the pure solvent were subtracted from the data collected.[13]

All our fits of the kinetic curves involved the temporal instrumental function taking into regard the cell thickness and hence the dispersion of the delay between the pump and the probe, originating from different group velocities of pump and probe pulses in the sample. The pump−probe cross-correlation function, unaffected by dispersion, was determined based on the two-photon absorption in the BK7 glass plate (excitation at

TABLE 1: NMR Data for the Reference Compounds 4 (Az-ref) and 7 (ZnP-ref) and the Dyad 6 (Az−ZnP)

product	yield (%)	^{1}H NMR, δ, J (Hz)[a]
4	96	2.16 (s, 3H, 6-$CH_2OC(O)CH_3$), 5.26 (s, 2H, 6-$CH_2OC(O)CH_3$), 7.20 (d, J = 10.2, 2H, C5-H and C7-H), 7.40 (d, J = 3.6, 2H, C1-H and C3-H), 7.92 (t, J = 3.6, 1H, C2-H), 8.33 (d, J = 10.2, 2H, C4-H and C8-H)
6	75	4.95 (s, 2H, −$OCH_2C(O)O$−), 5.47 (s, 2H, −$CH_2C(O)O$−), 7.20−7.32 (4H, C5-H, C7-H azulene and arom), 7.35 (d, J = 3.9, 2H, C1-H and C3-H azulene), 7.68−7.84 (m, 9H, arom), 7.87 (t, J = 3.9, 1H, C2-H azulene), 8.08−8.4 (10H, C4-H, C8-H azulene and arom), 8.86−9.06 (m, 8H, β-pyrrole)
7	82	3.95 (s, 3H, −OCH_3), 4.94 (s, 2H, −$OCH_2C(O)$−), 7.22−8.95 (27H, β-pyrrole and arom)

[a] ^{1}H NMR spectra were recorded on Varian Mercury Plus 300 MHz with TMS as internal standard and $CDCl_3$ as solvent.

400 nm); its fwhm is 150 fs. The real instrumental function used for the convolution with the kinetic exponential functions was determined separately for each wavelength, according to the theory presented in ref 14. It should be noted that the dispersion in the sample cell is especially important when 270 nm pump pulses were used. For example, the delay between pump and probe transit times after passage through the 2 mm sample cell filled with acetonitrile is 540 fs for a probe wavelength of 350 nm and 840 fs for a probe wavelength of 500 nm. This is much greater than the duration of the dispersion-free pump−probe cross-correlation function (150 fs). In such cases the temporal instrumental function is affected mostly by the dispersion delay in the sample cell, not by the pulse duration, and assumes a characteristic hatlike shape.[14] Thus, the temporal resolution in our transient absorption experiments was better for 400 nm excitation (about 100 fs) than for 270 nm excitation (about 500 fs).

3. Results and Discussion

3.1. Steady-State Measurements. The steady-state absorption and fluorescence spectra (excitation at 270 nm) of the reference compounds Az-ref and ZnP-ref in acetonitrile are shown in Figure 1, panels a and b. The maximum of the Soret absorption band for ZnP-ref occurs at 422 nm, while the maxima of the visible Q-bands are located at 557 and 597 nm. The emission spectrum for ZnP-ref is characterized by band maxima at 440 (S_2 emission), 603, and 656 nm (S_1 emission). The absorption spectrum of Az-ref shows a broad S_0-S_1 absorption band in the 500−700 nm region, a S_0-S_2 absorption band with a maximum at 344 nm, and a strong S_0-S_3 absorption band with two distinctive peaks at 282 and 277 nm. A fluorescence maximum corresponding to emission from the S_2 state of Az-ref is observed at 380 nm.

Figure 1c shows the steady-state absorption and fluorescence spectra (excitation at 270 nm) of the Az−ZnP dyad in acetonitrile. The absorption spectrum is essentially a sum of the spectra of the individual reference compounds (i.e., Az-ref and ZnP-ref). This indicates the absence of a strong ground-state electronic interaction between the two chromophores in the dyad molecule. Upon excitation at 270 nm, the fluorescence spectrum of the Az−ZnP dyad displays emission maxima at 380, 440, 603, and 656 nm. The emission band at 380 nm is ascribed to S_2 emission from the Az moiety, and the rest of the bands to either S_2 (λ_{em} = 440 nm) or S_1 (λ_{em} = 603 and 656 nm) emission from the ZnP moiety. The fluorescence spectra of Az-ref, ZnP-ref, and Az−ZnP presented in Figure 1 were obtained from sample solutions of similar concentrations (ca. 4 × 10^{-5} M), and are on the same relative scale.

The emission intensities of bands due to the ZnP chromophore in either the ZnP-ref or dyad are diminished by the reabsorption effect. This is especially true of the S_2 emission band at 440 nm, which overlaps strongly with the strong Soret absorption band. Furthermore, the intensities at maxima 603 and 656 nm are the same when measured with reabsorption minimized on the Edinburgh Instruments spectrofluorimeter. Regretably, quantitative results could not be obtained from this instrument due to laser photolysis of the dyad molecules. The emission spectra and fluorescence decay times (vide infra) of the solutions that exhibit photodecomposition contain features that are similar to those of the individual reference compounds, suggesting that the dyad undergoes simple scission of the tether connecting the two chromophores. A semiquantitative analysis suggests that the quantum yield of photodecomposition is small, but the rate of decomposition is nevertheless significant with the laser excitation system used on this instrument. Fortunately, accurate

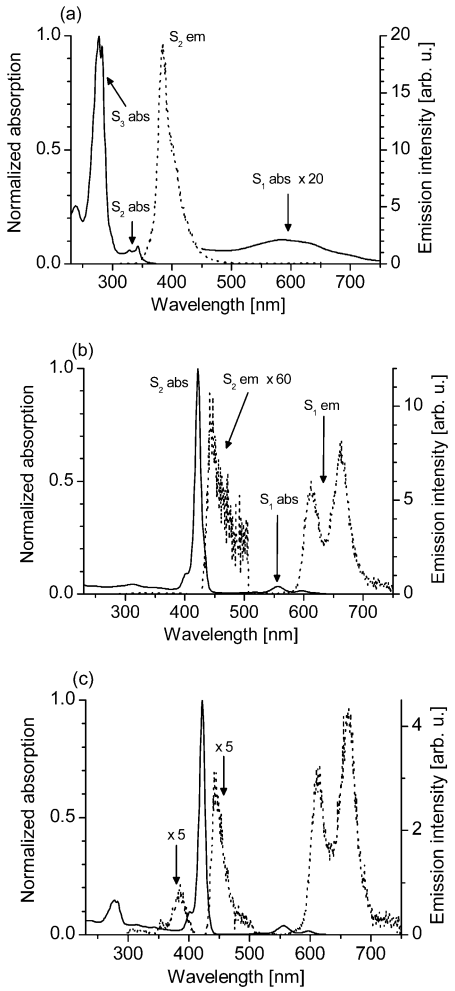

Figure 1. The normalized absorption (—) and emission (···) spectra for (a) Az-ref, (b) ZnP-ref, and (c) Az−ZnP dyad in acetonitrile. Abs is the absorption band, while em is the emission band. The absorption spectra of Az-ref and ZnP ref are independently normalized and the emission intensity scale is the same in all three panels, a, b, and c.

relative emission intensity and quantum yield measurements, comparing the dyad and the reference compounds, could be obtained using the MPF-3 spectrofluorimeter (polychromatic source) in which the rate of photodecomposition was small. In these experiments, fluorescence reabsorption occurs to the same extent when solutions of similar concentration are employed, so that accurate relative intensities can still be measured.

The molar extinction coefficients of Az-ref and ZnP-ref in acetonitrile at 270 nm were determined to be 3.82×10^4 and 1.62×10^4 M^{-1} cm^{-1}, respectively. At the same concentrations (ca. 4×10^{-5} M), the Az and ZnP moieties of the dyad absorb a smaller fraction of the incident light intensity (at 270 nm) than their respective reference compounds. The fraction of intensity of the light absorbed by the individual chromophores, *X*, of the dyad is obtained using the following equation:

$$F_X = \frac{A_X}{A_{Az} + A_{ZnP}}(1 - 10^{-(A_{Az}+A_{ZnP})}) \quad (1)$$

where *X* is either Az or ZnP, and $A_{Az\ (ZnP)}$ is the absorbance of Az (ZnP) at 270 nm. For quantitative comparison purposes, the emission band intensities associated with each of the chromophores in Az−ZnP were corrected accordingly so that the dyad chromophore and its reference compound absorb equal incident light intensity.

Upon excitation at 270 nm, the fluorescence intensity of the dyad Az ($\lambda_{em} = 380$ nm) is greatly reduced compared with the reference compound (cf. Figure 1). The S_2 emission quantum yield of Az in the dyad is ∼160 times smaller than Az-ref (Φ_{S_2}(Az-ref) = 0.032) in acetonitrile. The most likely process by which the excited S_2 state of the Az moiety of the dyad is efficiently quenched is electronic energy transfer to the S_2 state of the ZnP chromophore. Indeed a ∼3.2-fold enhancement in the S_2 fluorescence intensity of the dyad ZnP (at 440 nm in Figure 1c) is observed compared with ZnP-ref (Figure 1b).

The S_1-S_0 fluorescence, in the 550−750 nm range, of the dyad ZnP (Figure 1c) is quenched with respect to that of the ZnP-ref (Figure 1b). At $\lambda_{ex} = 270$ nm, the S_1 emission intensity of ZnP-ref is reduced 1.8-fold when connected to an Az chromophore in the dyad. At the same sample concentrations, a larger proportion (∼3.2 times from the emission intensity ratio of S_2 dyad to S_2 ZnP-ref) of excited dyad Az−ZnP molecules is created from both direct excitation (at 270 nm) and energy transfer from the Az moiety compared with the ZnP-ref. When considering an equivalent number of excited ZnP molecules, the S_1 ZnP emission quantum yield for the dyad is reduced 5.8-fold (1.8×3.2) compared with the reference compound (Φ_{S_1}(ZnP-ref) = 0.029). This is in agreement with the S_1 emission quenching effects observed at $\lambda_{ex} = 556$ nm where the S_1 state of the dyad ZnP is exclusively excited, and no S_2-S_2 energy transfer exists between the two chromophores. In this case, a 5.6-fold reduction in the S_1 fluorescence quantum yield for the dyad ZnP is observed compared with ZnP-ref. A deactivation pathway for the excited S_1 state of ZnP in the dyad involves S_1-S_1 energy transfer to Az. The electronic energy transfer efficiency, *E*, calculated using

$$E = 1 - \frac{\Phi_{S_1}(\text{dyad-ZnP})}{\Phi_{S_1}(\text{ZnP-ref})} \quad (2)$$

where Φ_{S_1}(dyad-ZnP) and Φ_{S_1}(ZnP-ref) are the S_1 emission quantum yields of the dyad ZnP and ZnP-ref, respectively, is 83%. A cyclic energy transfer process is therefore shown to occur in the dyad at $\lambda_{ex} = 270$ nm. This entails a forward S_2-S_2 energy transfer from Az to ZnP, followed by an S_2-S_1 internal conversion within the ZnP moiety, before a back S_1-S_1 energy transfer from ZnP to Az occurs.

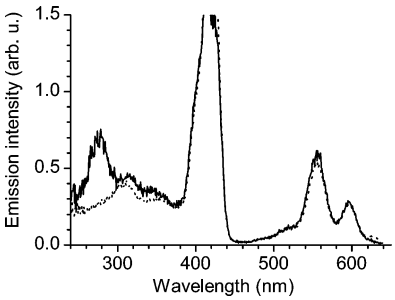

Figure 2. Excitation spectra ($\lambda_{em} = 660$ nm) of ZnP-ref (···) and Az−ZnP (—) in acetonitrile.

Further evidence of energy transfer from Az to ZnP in the dyad is provided from the fluorescence excitation spectra of Az−ZnP and ZnP-ref (see Figure 2). The excitation spectrum of ZnP-ref at $\lambda_{em} = 660$ nm is characterized by principal bands with maxima at 598, 558, and 422 nm and a relatively weak and broad band between 250 and 350 nm associated with upper ($n > 2$) excited states of ZnP. The normalized fluorescence excitation spectrum of Az−ZnP (Figure 2), monitored at $\lambda_{em} = 660$ nm, reveals bands arising from ZnP and an additional well-defined band with a maximum at 280 nm. The latter is attributed to the Az moiety, whereby excitation into the S_3 state of the Az leads to emission from the S_1 state of the ZnP, which can only be rationalized from the transfer of excitation energy from Az to ZnP in the dyad. The band in the excitation spectrum of the dyad associated with the S_2 state of Az, near 344 nm, is masked by the ZnP band and is therefore not apparent in the excitation spectrum of Az−ZnP. The ratio of the band intensities at 270 nm for Az−ZnP and ZnP-ref, after equalizing the incident light intensity absorbed by the two ZnP chromophores, is ∼3.4 (cf. the ratio of the molar extinction coefficients of Az−ZnP and ZnP-ref at 270 nm is also ∼3.4). This again suggests that following rapid, efficient Az S_3-S_2 internal conversion, efficient energy transfer (close to 100%) occurs from the S_2 state of Az to the S_2 state of ZnP in the dyad. The excited molecule then relaxes to the S_1 state of the ZnP moiety, which emits at 660 nm.

Similar types of quenching behavior were also observed in the nonpolar cyclohexane solvent. Upon excitation of Az−ZnP at 270 nm, a drastic reduction in the S_2 fluorescence intensity of the dyad Az (band maximum at 340 nm) and a concomitant increase in the S_2 fluorescence intensity of the dyad ZnP (band maximum at 430 nm) are observed when compared with their respective reference compounds. The S_2 emission quantum yield of the dyad Az is reduced ∼120-fold as a result of energy transfer to the S_2 state of the ZnP moiety. The S_1 emission intensity of the dyad ZnP chromophore is quenched ∼2.3-fold compared with the reference compound (maxima at 600 and 645 nm). The normalized fluorescence excitation spectrum of Az−ZnP (measured at $\lambda_{em} = 642$ nm) shows bands that are identical to the reference ZnP and an extra well-defined band at 280 nm arising from the S_3 state excitation of Az. The ratio of the intensity of the excitation spectra at 270 nm for Az−ZnP and ZnP-ref is ∼3.6, which corresponds well with the ratio of their molar extinction coefficients at the same absorption wavelength. When the number of excited dyad ZnP molecules, obtained from either direct excitation at 270 nm or energy transfer from Az, is matched with those of the ZnP-ref, the S_1 ZnP emission quantum yield of the dyad is found to be reduced 7.7-fold compared to the reference compound. This is in

TABLE 2: Fluorescence Decay Lifetimes for ZnP-ref, Az-ref, and Az−ZnP Obtained at Two Different Excitation Wavelengths, λ_{Ex}[a]

	λ_{ex} = 400 nm		λ_{ex} = 270 nm	
	λ_{em} (nm)	τ (ps)	λ_{em} (nm)	τ (ps)
ZnP-ref	424	1.7	428	1.9
	600, 660	1600	603	1600
Az-ref			380	690
Az−ZnP	660, 660	290 (0.7), 1600 (0.3)	603	290 (0.7), 1600 (0.3)

[a] The numbers in parentheses are the fractions of the total emission having the corresponding lifetime, τ.

agreement with the results obtained at λ_{ex} = 546 nm where only the S_1 state of ZnP is excited. The S_1-S_1 back energy transfer efficiency between ZnP and Az is calculated to be 87% from eq 2.

3.2. Time-Resolved Fluorescence Measurements. To investigate the excited-state dynamics, the time-resolved fluorescence lifetimes of Az−ZnP and the reference compounds were evaluated at several excitation and emission wavelengths in acetonitrile. The single-exponential fluorescence decay of Az-ref (λ_{ex} = 270 nm and λ_{em} = 380 nm) yielded a lifetime of 690 ps. The S_1 fluorescence decay profiles of ZnP-ref measured at λ_{em} = 600 and 660 nm exhibited a lifetime of 1.6 ns (λ_{ex} = 400 nm). At λ_{ex} = 270 nm, the S_1 fluorescence lifetime of ZnP-ref (λ_{em} = 603 nm) is also 1.6 ns. The S_2 fluorescence lifetimes of ZnP-ref determined using 400 and 270 nm laser excitations are 1.7 ps (λ_{em} = 424 nm) and 1.9 ps (λ_{em} = 428 nm), respectively, and are equal within experimental error. The various fluorescence lifetime values for the reference compounds are summarized in Table 2.

The temporal fluorescence decay profile of Az−ZnP measured at λ_{ex} = 270 nm and λ_{em} = 380 nm is dominated by azulene-containing photoproducts, making reliable analysis difficult in this particular case. The absence of a rise time component in the S_2 fluorescent profile of the ZnP chromophore of the dyad (λ_{ex} = 270 nm and λ_{em} = 428 nm), which is best fitted to a monoexponential decay function with lifetime component similar to that of ZnP-ref, implies that the intramolecular S_2-S_2 electronic energy transfer rate between Az and ZnP in the dyad is too fast to be detected by the time resolution of our current experimental setup (i.e., <1 ps).

The S_1-S_1 energy transfer dynamics from ZnP to Az was studied by exciting Az−ZnP at 270 nm and measuring the emission decay at 603 nm. The decay profile was analyzed as a sum of two exponentials that yielded a short lifetime component of 290 ps (70%) and a long lifetime component of 1.6 ns (30%). The latter is attributed to emission from free ZnP produced by laser photolysis of a fraction of the dyad. The short decay time of 290 ps is assigned to emission from the excited S_1 state of intact dyad ZnP quenched by intramolecular energy transfer to the S_1 state of the Az moiety. The energy transfer efficiency is calculated from eq 2 by replacing Φ_{S_1}(dyad-ZnP) with τ_{S_1}(dyad-ZnP) and Φ_{S_1}(ZnP-ref) with τ_{S_1}(ZnP-ref) where τ_{S_1}(dyad-ZnP) and τ_{S_1}(ZnP-ref) are the S_1 emission lifetimes of the dyad ZnP (290 ps) and ZnP-ref (1.6 ns), respectively. A value of E = 82% is obtained from the time-resolved measurements, which is in excellent agreement with the steady-state result. The rate of S_1-S_1 electronic energy transfer is calculated to be 2.8×10^9 s^{-1} using the following expression:

$$k_{eet} = \frac{1}{\tau_{S_1}(\text{dyad-ZnP})} - \frac{1}{\tau_{S_1}(\text{ZnP-ref})} \qquad (3)$$

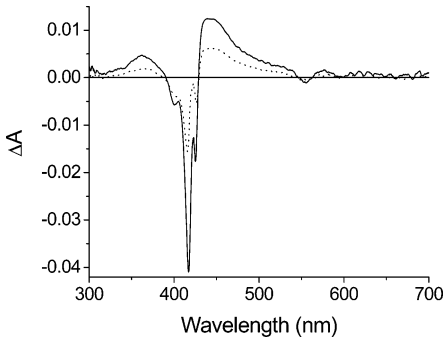

Figure 3. Transient absorption spectra of ZnP-ref (···) and Az−ZnP (—) in acetonitrile with 270 nm excitation and a 7 ps probe delay.

At λ_{ex} = 400 nm, the Az−ZnP dyad displays dual fluorescence lifetimes of 290 ps and 1.6 ns when emission was monitored at 600 nm (or 660 nm), suggesting no change in the energy transfer rate at the two excitation wavelengths (i.e., 270 and 400 nm).

In nonpolar cyclohexane, ZnP-ref decays with a monoexponential lifetime of 1.9 ns (λ_{ex} = 270 nm and λ_{em} = 639 nm). The forward S_2-S_2 energy transfer rate in the dyad is beyond the time resolution of our instrument and was therefore not measurable. The S_1 fluorescence decay of dyad-ZnP (λ_{ex} = 270 nm and λ_{em} = 639 nm) is fitted satisfactorily to a double-exponential decay function with lifetimes of 370 ps and 1.9 ns. The former is assigned to the quenched lifetime of intact ZnP in the dyad molecule, while the latter is again attributed to emission from free ZnP produced from laser photolysis of the dyad. The back S_1-S_1 energy transfer efficiency from ZnP to Az in the dyad is 81%, and the transfer rate is 2.2×10^9 s^{-1} (eq 3). This energy transfer rate is only slightly smaller than the one in acetonitrile and implies little solvent dependence on the k_{eet} values. The lack of solvent dependence suggests that the conformation of the dyad is similar in the two solvents.

3.3. Transient Absorption Measurements. The transient absorption spectrum of Az-ref recorded by exciting the compound at 270 nm was too weak to provide an analyzable signal. This stems from the small extinction coefficients of the transient species of azulene. In this case, the S_2-S_2 energy transfer process can be detected as a potential rise time in the ZnP transient spectrum, provided the transfer rate is slower than the temporal resolution of the instrument. Though Foggi et al.[15] have obtained femtosecond transient spectra of azulene using sample concentrations ranging from 10^{-1} to 10^{-3} M, such high concentrations could not be employed in this study due to the limited solubility of the dyad in the solvents used and the need to avoid dyad aggregation.

Figure 3 shows the transient absorption spectrum of ZnP-ref recorded 7 ps after excitation at 270 nm (2 μJ/pulse). The spectrum measured at a pump wavelength of 400 nm (10 μJ/pulse) shows the exact same features. Only the excited S_1 state of ZnP-ref persists after 7 ps, and the structure of the spectrum is characteristic of those previously reported for S_1-S_n absorptions of zinc tetraphenylporphyrin.[16−18] In particular, the bleaching of the Q(1,0) absorption band is seen at 560 nm, while the bleaching of the Q(0,0) band at 600 nm suffers from low signal intensity (Figure 3). However, this bleaching is more prominent when a higher pump pulse energy at 400 nm is used. It should be noted that in the 410−425 nm region the spectrum suffers from diminished probe light intensity due to the high absorbance of the ZnP-ref Soret band.

The transient absorption profiles of ZnP-ref obtained at pump wavelengths of 270 and 400 nm show similar kinetics when probed at the same wavelength. Three representative profiles

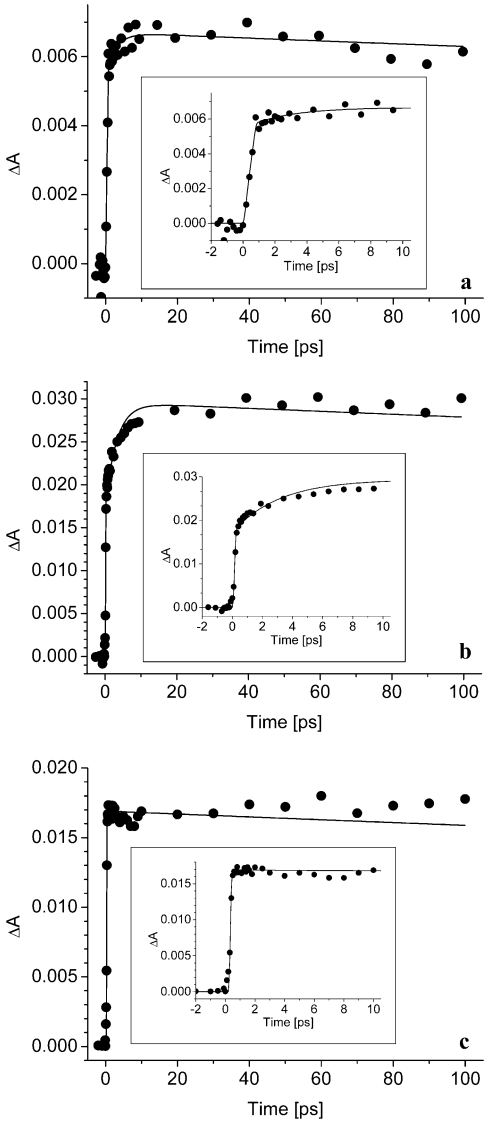

Figure 4. Transient absorption kinetics for ZnP-ref in acetonitrile: (a) pump wavelength = 270 nm and probe wavelength = 450 nm; (b) pump wavelength = 400 nm and probe wavelength = 450 nm; (c) pump wavelength = 400 nm and probe wavelength = 370 nm. The early portion of the transient is shown in greater detail in the inset.

recorded at probe wavelengths 450 and 370 nm are displayed in Figure 4. In each case, only the first 100 ps of the profile is shown in detail. The transient absorption trace at a pump wavelength of 270 nm and probe wavelength of 450 nm (Figure 4a) shows a rise characterized by a 3.0 ps time constant; the long-lived decay component (not shown) is arbitrarily fixed to the fluorescence lifetime of the S_1 state of ZnP-ref (i.e., 1.6 ns). The transient absorption trace at pump wavelength 400 nm and probe wavelength 450 nm (Figure 4b) displays similar features with a rise time of 2.5 ps, followed by a slow decay, which is again fixed to 1.6 ns. The short component seen in Figure 4, panels a and b, tracks the changes in the transient absorption as the molecule undergoes S_2-S_1 internal conversion, and the two values obtained (2.5 and 3.0 ps) are within experimental error. This is consistent with the S_2 emission lifetime value measured using time-resolved fluorescence measurements (see section 3.2).

The time evolution profile of the transient absorption at a probe wavelength of 370 nm following excitation with a 400 nm laser pulse (Figure 4c) does not change significantly in the first few picoseconds. Instead it decays slowly over 1−2 ns, which again corresponds to the S_1 decay of ZnP-ref. This suggests that the extinction coefficients for S_2-S_n and S_1-S_n transitions are similar at this probe wavelength, and a short lifetime component corresponding to the S_2-S_1 internal conversion is therefore not observed.

Transient absorption measurements were also performed on the dyad Az−ZnP in acetonitrile, and the spectrum at 7 ps after excitation with pump wavelength 270 nm is shown in Figure 3. We note from Figure 3 that at similar sample concentrations (ca. 4×10^{-5} M), the signal intensity for Az−ZnP is larger than that for ZnP-ref such that the average ratio at the maxima of the positive bands is ∼2.3. This ratio value increases to 3.2 when the fraction of incident light intensity absorbed by the dyad is corrected based on eq 1. This is also seen at different delay times and is indicative of a larger number of populated dyad ZnP S_1 states compared to the reference compound (i.e., ∼3.2 times, in agreement with steady-state measurement results discussed in section 3.1) resulting from intramolecular S_2-S_2 energy transfer within Az−ZnP. We also noted that laser photolysis of the dyad is significantly reduced by the use of a flow cell in these transient absorption measurements.

The transient absorption kinetic profile for Az−ZnP at a pump wavelength of 270 nm and a probe wavelength of 450 nm (Figure 5a) requires 3.3 ps rise and ∼300 ps decay components to adequately fit the data. When the probe wavelength is tuned to 370 nm (Figure 5b), the kinetic profile displays a single-exponential decay with a time constant of ∼300 ps. The 3.3 ps time constant observed at probe wavelength 450 nm is ascribed to the time taken for internal conversion to occur from the S_2 state of the dyad ZnP, while the ∼300 ps time constant at both probe wavelengths (370 and 450 nm) is attributed to a faster (than for ZnP-ref) relaxation of the excited S_1 state of dyad ZnP via energy transfer to the S_1 state of dyad Az. This is consistent with the time-resolved fluorescence measurement results discussed in section 3.2. We note that no temporal components in these kinetic profiles of these transients can be assigned to the rapid S_2-S_2 energy transfer process within the dyad. This suggests that the energy transfer from the Az moiety to the ZnP moiety occurs in a time scale shorter than the temporal resolution of our transient absorption instrument (i.e., <500 fs).

The transient absorption kinetic profile of Az−ZnP at a pump wavelength of 400 nm and a probe wavelength of 450 nm is shown in Figure 5c. At this excitation wavelength, S_2-S_2 energy transfer does not take place. The kinetic trace is described by a short 2.3 ps time component and a long ∼300 ps time component, consistent with the lifetime values obtained at a pump wavelength of 270 nm and probing at the same wavelength (Figure 5a). This confirms that when the dyad is excited at 270 nm, an ultrafast forward S_2-S_2 energy transfer process (<500 fs) occurs in the dyad, followed by a much slower S_1-S_1 back energy transfer. The latter is independent of the excitation wavelength and is shown to take place within ∼300 ps.

The transient absorption spectra of the Az−ZnP dyad and ZnP-ref in cyclohexane, measured with a pump wavelength of 270 nm, have similar features to those in acetonitrile. The positive Az−ZnP signal is ca. 3.5 times larger than that of the reference compound and supports the notion that extra dyad ZnP chromophores are excited by energy transfer from the Az moiety. In these experiments, in contrast to those in which acetonitrile was used as a solvent, the lower solubility of the dyad resulted in a significantly smaller transient absorption signal. Quantitative kinetic fits were only obtained in the region

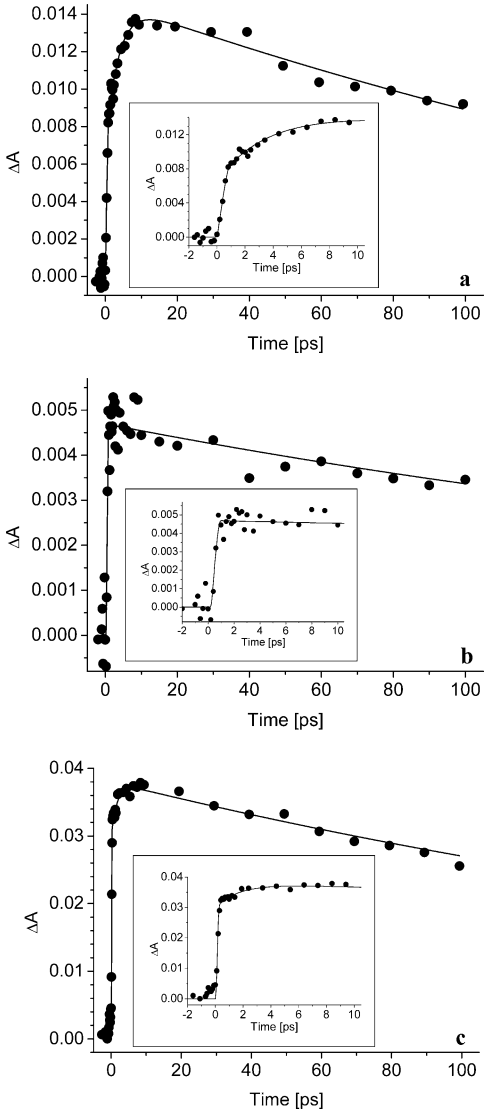

Figure 5. Transient absorption kinetics for Az−ZnP in acetonitrile: (a) pump wavelength = 370 nm and probe wavelength = 450 nm; (b) pump wavelength = 270 nm and probe wavelength = 450 nm; (c) pump wavelength = 400 nm and probe wavelength = 450 nm. The early portion of the transient is shown in greater detail in the inset.

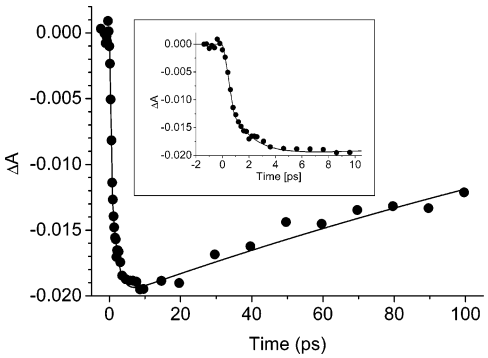

Figure 6. Transient absorption kinetics for Az−ZnP in cyclohexane with pump wavelength = 270 nm and probe wavelength = 420 nm. The early portion of the transient is shown in greater detail in the inset.

of the bleaching band where the signal was not affected by the high Soret band absorbance of the ZnP chromophore. A representative transient absorption kinetic profile of Az−ZnP at a probe wavelength of 420 nm (presented in Figure 6) decays with a time constant of 1.7 ps followed by a recovery with a time constant of ∼300 ps. The 1.7 ps component is again attributed to the S_2-S_1 internal conversion in cyclohexane and the longer component to the back S_1-S_1 energy transfer process. In cyclohexane, the forward S_2-S_2 energy transfer is again too rapid ($>2 \times 10^{12}$ s^{-1}) to be detected and occurs in a time scale of <500 fs.

3.4. Energy Transfer Dynamics. The rate of singlet−singlet energy transfer between the donor D and the acceptor A is often written in the form derived by Förster:[19]

$$k_{eet}^{F} = \left(\frac{1}{\tau_D}\right)\left(\frac{R_o}{R}\right)^6 \tag{4}$$

where τ_D is the fluorescence lifetime of D in the absence of A, R is the distance between D and A, and R_o is the critical distance where the transfer probability equals the emission probability. R_o is defined by

$$R_o^{\,6} = \frac{9000(\ln 10)\kappa^2 \Phi_D J(\tilde{\nu})}{128\pi^5 N \eta^4} \tag{5}$$

where Φ_D is the fluorescence quantum yield of D, N is Avogadro's number, η is the refractive index of the solvent, $J(\tilde{\nu})$ is the spectral overlap integral of the emission of D with the absorption of A, and κ^2 is the orientation factor defined by

$$\kappa^2 = (\cos\theta_T - 3\cos\theta_D \cos\theta_A)^2 \tag{6}$$

where θ_T is the angle between the transition moments of D and A and $\theta_{D\,(A)}$ is the angle between the transition moments of D (A) and the line connecting their centers. Mårtensson's method[20] was employed to calculate the average orientation factor, $\langle\kappa\rangle^2$, for a system consisting of a chromophore of 4-fold symmetry (i.e., the ZnP moiety). By assuming that the orientation of the various transition moments of azulene are not significantly affected by the tethering substituent, the S_0-S_1 and S_0-S_2 transitions are taken to be polarized along the short and long axis of the azulene molecule, respectively. Using the known geometries of ZnP and Az and the energy-minimized structure of the tether connecting these two moieties (Hartree−Fock with a 3-21G* basis set using Spartan '04, Wavefunction Inc.), the calculated average orientation factors for the forward S_2-S_2 and back S_1-S_1 energy transfer processes are 1.56 and 0.035, respectively. The center-to-center separation of the chromophores R is taken to be 14.4 Å.

The rate of Förster S_1-S_1 energy transfer from dyad ZnP to dyad Az, in acetonitrile, determined from eqs 4 and 5 (using PhotochemCAD[21]) is 7.5×10^7 s^{-1} (3.9×10^{-15} cm^6/mmol). The experimental energy transfer rate (i.e., $k_{eet} = 2.8 \times 10^9$ s^{-1}) is ca. 40 times faster than predicted assuming the Förster mechanism. One simple rationale is that the conformation of the active electronic energy transfer species is not the extended one but rather one with $R \approx 8$ Å that is independent of solvent polarity. However, if the extended conformation is dominant, then this suggests that other energy transfer mechanisms are also operative in the dyad system. One such mechanism, proposed by Dexter,[22] involves the short-range orbital overlap interaction between the energy donor and acceptor chromophores, and the energy transfer rate is given by[23]

$$k_{eet}^{D} = \frac{2\pi}{\hbar} K J_D \exp(-2R_e/L) \tag{7}$$

where L is the average Bohr radius and J_D is the integral overlap between donor fluorescence and acceptor absorption spectra. The edge-to-edge displacement (R_e) between the Az and ZnP

moieties in the dyad is <7 Å, which means that they are close enough to bring the Dexter mechanism into effect. Furthermore, J_D (1.6×10^{-4} cm) is relatively high, which encourages the augmentation of the energy transfer rate by the Dexter mechanism. Another orbital-overlap-dependent interaction term involving the coupling between ionic charge transfer configurations and locally excited states (i.e., through-configuration interaction) has also been shown to be important.[24]

When the separation between D and A approaches the size of the chromophores, as is the case for Az−ZnP, higher order Coulombic terms and the contributions described by the distributed transition-monopole theory may also play a significant role in accounting for the energy transfer rate.[25,26] The parameters required for the evaluation of these two mechanisms are often not easily extracted from measured spectroscopic data, and this renders any quantitative analysis difficult. Superexchange through-bond-mediated energy transfer via the spacer between the ZnP and Az moieties can also contribute significantly to the energy transfer process. Its importance will be further tested by using spacer groups of different length and structure.

The Förster S_2-S_2 energy transfer rate from dyad Az to dyad ZnP in acetonitrile is calculated (from PhotochemCAD) to be 2.2×10^{11} s^{-1} ($J(\tilde{\nu}) = 1.0 \times 10^{-13}$ cm^6/mmol), while the actual transfer rate is $>2 \times 10^{12}$ s^{-1}. The Förster rate suggests that the S_2 lifetime of the quenched dyad Az is 4.4 ps, which cannot be experimentally resolved from the S_2 lifetime of the dyad ZnP. However, the absence of a rise component of ca. 4 ps in the time-resolved fluorescence profile of the S_2 state of dyad ZnP, and the absence of a ca. 4 ps component in the transient absorption kinetic trace of Az−ZnP at pump wavelength 270 nm and probe wavelength 370 nm also strongly indicate that Förster mechanism does not adequately describe the actual energy transfer dynamics. The several mechanisms present in the S_1-S_1 energy transfer process work in parallel and are also in operation here. The Förster critical distance in eq 4 does not change significantly in the two solvents employed. For the S_2-S_2 energy transfer process, R_o is 33.5 Å in both acetonitrile and cyclohexane, and for the S_1-S_1 energy transfer process, R_o is 10.1 Å in acetonitrile and 9.3 Å in cyclohexane ($k_{eet}^F \approx 4 \times 10^7$ s^{-1}). These similarities in the R_o values, together with the similar dyad relaxation rates observed in cyclohexane and acetonitrile, suggest that the conformation of the dyad is independent of the polarity of the aprotic solvent and that the same relaxation mechanism is operative in both solvents. However, in both solvents, the rapid energy transfer rates observed cannot be rationalized using the Förster mechanism, and it is therefore necessary to invoke other processes (e.g., the Dexter mechanism) to account for the discrepancy.

The possible role of electron transfer in the quenching of the S_2 and S_1 states of dyad Az and ZnP, respectively, in acetonitrile can be assessed by calculating the Gibbs free energy change ($\Delta G°$) involved in the charge separation process:

$$\Delta G° = E_{ox} - E_{red} - E_{oo} - (Ne^2/(\epsilon R)) \qquad (8)$$

We first examine the electron-transfer process from Az to ZnP in the dyad. The redox potentials of azulene and zinc tetraphenylporphyrin in acetonitrile were assigned to Az-ref and ZnP-ref, respectively, without loss of generality. The oxidation potential of Az-ref is thus $E_{ox} = 0.88$ V, while the reduction potential of ZnP-ref is $E_{red} = -1.30$ V.[6] The energy of the Az-ref S_2 state ($E_{oo} = 3.4$ eV) is estimated by averaging the energies of the absorption and corresponding emission maxima. The work

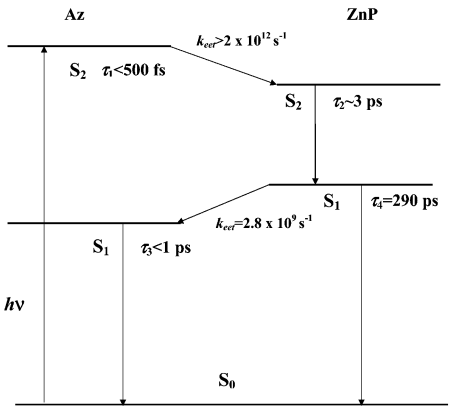

Figure 7. Energy levels (nts) of the Az and ZnP moieties in the Az−ZnP dyad and the major EET and decay pathways.

term ($Ne^2/(\epsilon R)$) containing the relative permittivity parameter (ϵ) is 0.03 eV, and the $-\Delta G°$ value evaluated from eq 8 is therefore 1.25 eV in acetonitrile. A fast electron-transfer reaction is known to take place in the activationless area when $-\Delta G°$ is close to the total reorganization energy λ (i.e., $-\Delta G° \approx \lambda$). For rigid molecules (e.g., porphyrins) in polar solvents, the λ value is often smaller than 1 eV. Therefore, the electron-transfer process from Az to ZnP in the dyad should fall in the Marcus inverted region ($-\Delta G° > \lambda$) and thus would be too slow to account for the efficient quenching of the S_2 state of dyad Az. Makinoshima et al.[27] and Kesti et al.[28] have also reported slow electron-transfer procesess (inverted region) from either S_2 azulene or S_2 zinc porphyrin to C_{60}, based on the calculated $\Delta G°$ values. In both studies, a purely charge-separation mechanism was found to be inadequate to explain the quenching dynamics of the donor molecule.

The driving force for electron transfer from S_1 ZnP to Az in acetonitrile is calculated to be $\Delta G° = 0.32$ eV, using the parameters $E_{ox} = 0.80$ V for ZnP-ref,[29] $E_{red} = -1.65$ V for Az-ref,[30] and $E_{oo} = 2.1$ eV for the energy of the S_1 ZnP-ref. The positive $\Delta G°$ indicates that electron transfer from S_1 dyad ZnP to Az is not thermodynamically feasible.

The $\Delta G°$ values for electron transfer in cyclohexane are evaluated using eq 8 with a correction term included to account for the different dielectric constant of cyclohexane from the reference solvent (acetonitrile). The positive $\Delta G°$ evaluated for charge separation between S_2 Az and ZnP and between S_1 ZnP and Az are 0.43 and 2.0 eV, respectively. Therefore, in nonpolar cyclohexane, intramolecular electron-transfer cannot take place from either the S_2 state of dyad Az or the S_1 state of dyad ZnP. This complements the finding that the observed excited state decay rates are independent of solvent polarity and are attributable exclusively to electronic energy transfer.

4. Conclusion

We have investigated the dynamics of cyclic energy transfer in a covalently tethered azulene-zinc porphyrin dyad. Upon excitation of the S_2 state of the Az moiety, ultrafast energy transfer ($k_{eet} > 2 \times 10^{12}$ s^{-1}) to the S_2 state of the ZnP moiety takes place in acetonitrile (see Figure 7). The ZnP in its S_2 state subsequently undergoes rapid internal conversion to its S_1 state. Thereafter, the excitation residing on the S_1 state of the ZnP is returned to the Az via an efficient back S_1-S_1 energy transfer ($k_{eet} = 2.8 \times 10^9$ s^{-1}). The cyclic energy transfer rates (S_2-S_2 and S_1-S_1 rates are $>2 \times 10^{12}$ and 2.2×10^9 s^{-1}, respectively) do not vary significantly in cyclohexane. In both solvents, Förster theory is inadequate in explaining the efficient energy

transfer dynamics, and other processes such as the Dexter mechanism must be invoked.

Acknowledgment. We thank James Hutchison and Professor Ken Ghiggino (University of Melbourne) for doing preliminary experiments on this system. Spectroscopic measurements were performed at the Center for Ultrafast Laser Spectroscopy, A. Mickiewicz University, Poznan, Poland. R.P.S. and E.K.L.Y. thank the Natural Sciences and Engineering Research Council of Canada for financial support. A.M., J.K., and M.Z. thank the State Committee for Scientific Research, Poland, Project 4 T09A 166 24, for financial support.

References and Notes

(1) Burdzinski, G.; Kubicki, J.; Maciejewski, A.; Steer, R. P.; Velate, S.; Yeow, E. K. L. In *Molecular and Supramolecular Photochemistry − Organic Photochemistry Part II*; Ramamurthy, V., Schanze, K. S., Eds.; Marcel Dekker: New York, 2004, in press.

(2) Tétreault, N.; Muthyala, R. S.; Liu, R. H. S.; Steer, R. P. *J. Phys. Chem. A* **1999**, *103*, 2524.

(3) Kobayashi, H.; Kaizu, Y. In *Porphyrins: Excited States and Dynamics*; Gouterman, M., Rentzepis, P. M., Straub, K. D., Eds.; American Chemical Society: Washington, DC, 1986; p 105.

(4) Remacle, F.; Speiser, S.; Levine, R. D. *J. Phys. Chem. B* **2001**, *105*, 5589.

(5) Yeow, E. K. L.; Steer, R. P. *Chem. Phys. Lett.* **2003**, *377*, 391.

(6) Yeow, E. K. L.; Steer, R. P. *Phys. Chem. Chem. Phys*. **2003**, *5*, 97.

(7) (a) Hafner, K.; Bernhard, C. *Angew. Chem*. **1957**, *69*, 393. (b) Estdale, S. E.; Bzettle, R.; Dunmur, D. A.; Marson, C. M. *J. Mater. Chem.* **1997**, *7* (3), 391.

(8) (a) Alder A. D.; Longo F. R.; Finarelli J. D. *J. Org. Chem*. **1967**, *32*, 476. (b) Little R. G.; Anton J. A.; Loach P. A.; Ibers J. A. *J. Heterocycl. Chem*. **1975**, *12* (2), 343. (c) Semeikin A. S.; Koyfman O. I.; Berezin B. D. *Khim. Heterotz. Soed. (Russ.)* **1982**, *10*, 1354.

(9) Karolczak, J.; Kowalska, D.; Lukaszewicz, A.; Maciejewski, A.; Steer, R. P. *J. Phys. Chem. A* **2004**, *108*, 4570.

(10) Karolczak, J.; Kubicki, J.; Komar, D.; Wrozowa, T.; Dobek, K.; Ciesielska, B.; Maciejewski, A. *Chem. Phys. Lett.* **2001**, *344*, 154.

(11) Maciejewski, A.; Naskrecki, R.; Lorenc, M.; Ziolek, M.; Karolczak, J.; Kubicki, J.; Matysiak, M.; Szymanski, M. *J. Mol. Struct.* **2000**, *555*, 1.

(12) Nakayama T.; Amijima Y.; Ibuki K.; Hamanoue K. *Rev. Sci. Instrum*. **1997**, *68*, 436.

(13) Lorenc, M.; Ziolek, M.; Naskręcki, R.; Karolczak, J.; Kubicki, J.; Maciejewski, A. *Appl. Phys. B* **2002**, *74*, 19.

(14) Ziolek, M., Lorenc, M.; Naskrecki, R. *Appl. Phys. B* **2001**, *72*, 843.

(15) Foggi, P.; Neuwahl, F. V. R.; Moroni, L.; Salvi, P. R. *J. Phys. Chem. A* **2003**, *107*, 1689.

(16) Rodriguez, J.; Kirmaier, C.; Holten D. *J. Am. Chem. Soc*. **1989**, *111*, 6500.

(17) Hayes, R. T.; Walsh, C. J.; Wasielewski, M. R. *J. Phys. Chem. A* **2004**, *108*, 2375.

(18) Enescu, M.; Steenkeste, K.; Tfibel, F.; Fontaine-Aupart, M.-P. *Phys. Chem. Chem. Phys*. **2002**, *4*, 6092.

(19) Förster, Th. *Discuss. Faraday Soc*. **1959**, *27*, 7.

(20) Mårtensson, J. *Chem. Phys. Lett*. **1994**, *229*, 449.

(21) Du, H.; Fuh, R.-C. A.; Li, J.; Corkan, L. A.; Lindsey, J. S. *Photochem. Photobiol.* **1998**, *68*, 141.

(22) Dexter, D. L. *J. Chem. Phys*. **1953**, *21*, 836.

(23) Speiser, S. *Chem. Rev*. **1996**, *96*, 1953.

(24) Yeow, E. K. L.; Ghiggino, K. P. *J. Phys. Chem. A* **2000**, *104*, 5825.

(25) Scholes, G. D.; Ghiggino, K. P. In *Advances in Multiphoton Processes and Spectroscopy*; Lin, S. H., Villaeys, A. A., Fujimura, Y., Eds.; World Scientific: Singapore, 1996; Vol. 10, p 95.

(26) Karvarnos, G. J. *Fundamentals of Photoinduced Electron Transfer*; VCH: New York, 1993.

(27) Makinoshima, T.; Fujitsuka, M.; Sasaki, M.; Araki, Y.; Ito, O.; Ito, S.; Morita, N. *J. Phys. Chem. A* **2004**, *108*, 368.

(28) Kesti, T.; Tkachenko, N.; Yamada, H.; Imahori, H.; Fukuzumi, S.; Lemmetyinen, H. *Photochem. Photobiol. Sci*. **2003**, *2*, 251.

(29) Morandeira, A.; Engeli, L.; Vauthey, E. *J. Phys. Chem. A* **2002**, *106*, 4833.

(30) Muller, P.-A.; Vauthey, E. *J. Phys. Chem. A* **2001**, *105*, 5994.